



# 1 The applications of UFS-Coastal v1.0.0b01: wave-current coupling of 2 SCHISM and WAVEWATCH III

3 Yunfang Sun<sup>1,2</sup>, Ufuk Turuncoglu<sup>3</sup>, Mansur Jisan<sup>4,5</sup>, Hao-Cheng Yu<sup>6</sup>, Joseph Zhang<sup>6</sup>, Carsten Lemmen<sup>7</sup>,  
4 Ali Abdolali<sup>8</sup>, Denise Worthen<sup>9</sup>, Ishan A Tsay<sup>3</sup>, Jana Haddad<sup>1,5</sup>, Panagiotis Velissariou<sup>1,11</sup>, Felicio  
5 Cassalho<sup>1,5</sup>, Soroosh Mani<sup>1</sup>, Fariborz Daneshvar<sup>1,5</sup>, Saeideh Banihashemi<sup>9</sup>, Ali Salimi-Tarazouj<sup>9</sup>, Joseph  
6 Smith<sup>10</sup>, Edward Myers<sup>1</sup>, Saeed Moghimi<sup>1</sup>

7  
8 <sup>1</sup>NOAA/Coast Survey Development Laboratory, Silver Spring, Maryland, USA

9 <sup>2</sup>Axiom Consultants Inc, Rockville, Maryland USA

10 <sup>3</sup>National Center for Atmospheric Research (NCAR), Boulder, Colorado, USA

11 <sup>4</sup>NOAA Center for Operational Oceanographic Products and Services, Silver Spring, Maryland, USA

12 <sup>5</sup>Ocean Associates Inc., Arlington, Virginia USA

13 <sup>6</sup>Virginia Institute of Marine Science (VIMS), William & Mary, Gloucester Point, Virginia USA

14 <sup>7</sup>Institute of Systems Analysis and Modeling, Helmholtz-Zentrum Hereon, Geesthacht, Germany

15 <sup>8</sup>US Army Engineer Research and Development Center Coastal and Hydraulics Laboratory, Vicksburg, Mississippi USA

16 <sup>9</sup>NOAA/National Centers for Environmental Prediction, College Park, Maryland, USA

17 <sup>10</sup>College of Earth, Ocean and Atmospheric Sciences, Oregon State University, Corvallis, Oregon USA

18 <sup>11</sup>NOAA/National Hurricane Center, Miami, Florida, USA

19

20 *Correspondence to:* Y. Sun (Yunfang.sun@noaa.gov)

## 21 Abstract

22 Accurate prediction of coastal flooding and nearshore processes requires a coupled modeling framework that resolves  
23 interactions among ocean circulation, surface waves, ice, and atmospheric forcing across complex coastal geometries. To  
24 address this need, we present Unified Forecast System Coastal model (UFS-Coastal), a coupled coastal modeling framework  
25 extending the Unified Forecast System Weather Model (UFS-WM). The UFS-Coastal was developed to address this need by  
26 disentangle extending the prior infrastructure (called CoastalApp), and combining CoastalApp and UFS-WM, and  
27 byintegrating four different coastal hydrodynamic models: SCHISM, ADCIRC, FVCOM, and ROMS, along with the spectral  
28 wave model WAVEWATCH III (WW3) and CICE within a unified coupled framework. Here we introduce UFS-Coastal to  
29 the community, and focus on one particular aspect, the wave-current coupling between SCHISM and WW3 with two methods:  
30 the Longuet-Higgins radiation stress formulation and a three-dimensional (3D) vortex approach. We provide a comprehensive  
31 description of UFS-Coastal's infrastructure, coupling methodologies, and its automated regression testing framework. The  
32 system's performance is demonstrated through experiments in the Duck, North Carolina (NC) region against Field Research  
33 Facility observations. Both wave-current coupling schemes between the SCHISM and WW3 could successfully reproduce  
34 observed coastal hydrodynamics and wave conditions; notably, the 3D vortex coupling improved simulations of wave-induced  
35 mixing in shallow and stratified environments. Overall, UFS-Coastal offers a robust framework for accurate prediction of



36 coastal flooding, storm surge events, and wave-current interactions, supporting both research and operational forecasting  
37 applications.

## 38 **1 Introduction**

39 Coastal zones present unique challenges for numerical modeling. Processes such as storm surge generation and propagation,  
40 wave transformation, tidal estuarine exchange, wetting-drying over coastal floodplains and wave current interaction (which  
41 shifts wave's infragravity, sea-swell and windwaves compare to the wave alone) require high horizontal and vertical resolution  
42 and specialized physical parameterizations (Deb et al., 2022). Existing global and regional numerical weather prediction and  
43 Earth system models typically lack the resolution and physics required to accurately represent these complex processes,  
44 particularly at the land-sea-wave interface (Ward et al., 2020; Gröger et al., 2021; Thomas et al., 2021; Abdolali et al., 2021)  
45 Accurate prediction of coastal flooding, estuarine dynamics, and nearshore wave transformation requires numerical models  
46 specifically designed for coastal environments, where horizontal scales can range from meters in tidal inlets to kilometers on  
47 the continental shelf.

48 The Unified Forecast System (UFS) is a comprehensive, community-supported modeling framework designed to provide  
49 seamless earth system prediction across spatial and temporal scale (Jacobs, 2021; Worthen et al., 2024). The UFS serves both  
50 operational and research applications, from global weather forecasting to regional and local hazard prediction, and supports  
51 coupled modeling across the atmosphere, ocean, land, sea ice, and waves (Worthen et al., 2024). The UFS-Weather Model  
52 (UFS-WM), the core configuration for numerical weather prediction, provides a coupled atmosphere-land-sea ice-ocean-wave  
53 system, but it was originally designed to support large-scale processes and does not explicitly resolve the complex dynamics  
54 necessary for accurate prediction of coastal and nearshore processes.

55 To address this gap and following the CoastalApp initiative from the National Oceanic and Atmospheric Administration  
56 (NOAA) 's Consumer Options for an Alternative System to Allocate Losses (COASTAL) Act program (COASTAL Act,  
57 2012), the UFS-Coastal was developed as an extension of the UFS-WM, specifically designed to enhance the modeling and  
58 prediction of coastal and nearshore processes. The UFS-Coastal extends the UFS-WM with the addition of four coastal ocean  
59 circulation models: (1) the Semi-implicit Cross-scale Hydroscience Integrated System Model (SCHISM), an unstructured-grid  
60 hydrodynamic model designed for cross-scale applications, particularly in estuaries and coastal regions with complex geometry  
61 (Zhang and Baptista, 2008; Zhang et al., 2016); (2) the Finite Volume Community Ocean Model (FVCOM), a finite-volume,  
62 unstructured-grid ocean model widely used for coastal and estuarine circulation, which emphasizes conservative transport  
63 (Chen et al., 2006; Chen et al., 2013); (3) the Advanced Circulation Model (ADCIRC), an unstructured-grid hydrodynamic  
64 model optimized for storm surge, tidal, and hurricane modeling (Luettich and Westerink, 2004; Moghimi et al., 2020a); and  
65 (4) the Regional Ocean Modeling System (ROMS), a structured-grid, terrain-following coordinate model used extensively for  
66 shelf-scale circulation and biogeochemical modeling (Shchepetkin and McWilliams, 2005; Moore et al., 2011).



67 These coastal ocean models are coupled within the UFS-Coastal, enabling them to interact dynamically with surface waves  
68 (via WAVEWATCH III® (WW3)) (The Wavewatch III® Development Group (WW3DG), 2019; Abdolali et al., 2020; Alves  
69 et al., 2024), and sea ice (via Community sea Ice Code (CICE)) (Rae et al., 2015), and also receive the atmospheric and oceanic  
70 forcings from the Community Data Models for Earth Prediction Systems (CDEPS) via the Community Mediator for Earth  
71 Prediction Systems (CMEPS). This architecture allows for two-way coupled simulations where atmospheric forcing drives  
72 coastal circulation and wave generation, while wave-modified stress and wave setup feed back to the hydrodynamic model.  
73 The inclusion of multiple coastal ocean models allows the UFS-Coastal to leverage the unique strengths of each, from the  
74 estuarine-scale flexibility of SCHISM and FVCOM to the storm surge capabilities of ADCIRC and the established physical  
75 parameterizations of ROMS.

76 This paper presents a comprehensive description of the UFS-Coastal architecture, including its infrastructure, component  
77 models, and coupling strategies, with a focus on the recent developments towards SCHISM and WW3 coupling configurations.  
78 Here we also describe the system's continuous integration and continuous deployment (CI/CD) and automated regression  
79 testing framework, designed to ensure stability and reproducibility as the system evolves. Finally, we present initial evaluation  
80 results from the series of test cases: Hurricane Sandy in the Duck, NC, leveraging nearshore observations made by U.S. Army  
81 Corps of Engineers (USACE) Engineer Research and Development Center (ERDC) at their Field Research Facility (FRF).  
82 These test cases illustrate the use of UFS Coastal to explore wave-current interactions in the nearshore, and highlight the  
83 advantages of coupled ocean-wave simulations driven by prescribed atmospheric forcing for improved prediction of storm-  
84 driven coastal flooding and nearshore circulation processes.

85 The paper is organized as follows: Section 2 describes the overall infrastructure of UFS-Coastal, including details of the model  
86 components and the coupling infrastructure. Section 3 presents the configuration and results of the experimental cases used to  
87 evaluate the system, with particular focus on Hurricane Sandy and the Duck, NC region. Section 4 discusses the results, and  
88 provides an outlook for future development and applications.

## 89 **2 UFS Coastal Infrastructure description**

90 The CoastalApp, a flexible and portable coastal modeling framework, was developed under NOAA's COASTAL Act program  
91 in 2017 (<https://github.com/noaa-ocs-modeling/CoastalApp>). The CoastalApp was developed by NOAA's National Ocean  
92 Service (NOS) Storm Surge Modeling Team and partners, and is hosted within the Office of Coast Survey's modeling GitHub  
93 organization (<https://github.com/noaa-ocs-modeling/>). It employs a coupled multi-model approach driven by the NOAA  
94 Environmental Modeling System (NEMS) and follows National Unified Operational Prediction Capability (NUOPC) best  
95 practices. It supported a wide range of coastal applications, including storm surge and wave modeling, with capabilities for  
96 both one-way and two-way coupled configurations (Moghimi et al., 2019; Moghimi et al., 2020b, a). To streamline efforts and  
97 align closely with NOAA's UFS, the NOS team deprecated CoastalApp in favour of developing UFS-Coastal, a fork of the  
98 UFS-WM. During this transition, the UFS-Coastal inherited the four specialized coastal hydrodynamic components originally



99 developed within CoastalApp: ADCIRC, FVCOM, SCHISM and ROMS, facilitating continuity in model capabilities and  
100 leveraging prior advances made under CoastalApp.

101 This transition introduced two key architectural changes: (1) the NEMS driver was replaced by the CMEPS, providing  
102 standardized regridding, flux calculation, and time management across components; and (2) the coastal models gained direct  
103 access to the UFS-WM's existing component suite, including FV3 atmosphere, land surface models, WW3, and CICE . The  
104 UFS-Coastal retained the four specialized coastal hydrodynamic models originally developed within CoastalApp (ADCIRC,  
105 FVCOM, SCHISM, and ROMS) while embedding them within this broader coupled framework (Fig. 1). External forcing data  
106 (e.g., atmospheric reanalysis, observed boundary conditions) is ingested through the CDEPS.

107 Building upon the foundational infrastructure provided by the UFS-WM and CoastalApp, the UFS-Coastal further enhances  
108 the capabilities for modeling coastal and estuarine environments by integrating these four specialized coastal ocean models  
109 (Fig. 1): the UFS-WM contributes core modeling components (including atmosphere, land surface, sea ice, and wave models)  
110 The UFS-Coastal offers enhanced spatial resolution, resolved accurate coastlines, improved wetting and drying capabilities,  
111 and physics tailored specifically for nearshore environments, providing users with significant flexibility to address diverse  
112 coastal modeling objectives, which are challenging in UFS-WM, even when using the same unstructured grid

113 The subsequent sections provide detailed descriptions of UFS-Coastal's infrastructure, components, and their practical  
114 applications.

## 115 **2.1 UFS-WM component descriptions**

### 116 **2.1.1 CDEPS and CMEPS**

117 CDEPS is constructed on the Earth System Modeling Framework (ESMF) and comprises a collection of NUOPC-compliant  
118 data components together with ESMF-based “stream” code. In essence, these data components ingest data from external sources,  
119 process and then send to other NUOPC compliant components such as CMEPS mediator. Because the fields passed to the  
120 mediator have the same form as those originating from an active component, neither the mediator nor any other CMEPS-  
121 compliant component needs to know whether a given component is fully active or merely supplying data. This CDEPS yields  
122 two important practical benefits: (1) regridding between the stream resolution and the model resolution is carried out at run  
123 time using whichever regridding options ESMF provides, and (2) Parallel I/O (PIO) library is leveraged in CDEPS so that  
124 stream data are read in parallel by the stream code (Worthen et al., 2024).

125 The external data sources that CDEPS interfaces with include (1) Atmospheric reanalysis products — for example, the European  
126 Centre for Medium-Range Weather Forecasts (ECMWF) Reanalysis v5 (ERA5) (Hersbach et al., 2020), and (2) Observed or  
127 pre-simulated surface fluxes, such as water levels derived from ocean observations or air-sea fluxes obtained from large-scale  
128 models, including the observed data from the USACE ERDC's Coastal and Hydraulics Laboratory's FRF (USACE, 2025).  
129 This capability is especially valuable when the UFS-WM/UFS-Coastal is applied to limited-area domains, which depend on  
130 realistic surface forcing drawn from other simulations or observational datasets. By treating external data streams in the same  
131 manner as internal component data streams, CDEPS preserves temporal and spatial consistency across the coupled system.



132 CMEPS is an ESMF/NUOPC-compliant mediator for coupling the components of Earth system models. It is presently used in  
133 a range of applications, among them the National Center for Atmospheric Research (NCAR) Community Earth System Model  
134 (CESM) and NOAA's UFS. The mediator conveys field information from one component to another, a process that may  
135 involve one or more operations on the exchanged fields, including the mapping of fields across component grids, the merging  
136 of fields from different components, and the time-averaging of fields over differing coupling periods. In this way, CMEPS  
137 absorbs the complex coupling operations while leaving the source code of each individual component model in the coupled  
138 system unchanged.

139 CMEPS provides several key functions, including:

- 140 1) **Regridding:** CMEPS maps fields between the structured atmospheric grid and the unstructured meshes used by  
141 SCHISM, FVCOM, ADCIRC, and WW3, or the structured grid used by ROMS, WW3, and CICE, applying a range  
142 of temporal and spatial interpolation methods.
- 143 2) **Time management:** CMEPS allows the coupling of components on different time intervals by synchronizing  
144 information exchange at the appropriate coupling intervals, so that atmosphere–ocean–wave interactions can evolve  
145 dynamically in time.
- 146 3) **Data exchange:** CMEPS manages the transfer of surface fluxes (wind stress, sea surface pressure), surface elevation,  
147 ocean currents, and wave parameters among the components.

148 The flexibility of CMEPS allows the UFS-Coastal to support configurable coupling intervals for different component pairs,  
149 enabling efficient simulations even in high-resolution, computationally intensive domains.

150 The combination of CMEPS and CDEPS allows the UFS-WM/UFS-Coastal to seamlessly integrate external forcing data (e.g.,  
151 reanalysis winds, global model forcing conditions) with dynamically evolving coupled simulations. CMEPS manages real-  
152 time interactions among the active components, while CDEPS ensures that prescribed external forcing is applied consistently  
153 at the domain. Together, these components allow the UFS-Coastal to operate flexibly across scales, from globally forced  
154 regional domains to fully coupled hurricane simulations with dynamic wave and surge feedback.

### 155 **2.1.2 WW3**

156 WW3 is a third-generation, phase-averaged spectral wave model that simulates the evolution of wave action density in  
157 frequency–direction space by solving the wave action balance equation (The Wavewatch III® Development Group (WW3DG),  
158 2019). Rather than resolving individual wave phases, WW3 parameterizes the key physical processes that govern wave  
159 evolution, including wind-driven wave growth, nonlinear quadruplet wave–wave interactions that redistribute energy across  
160 the spectrum, and dissipation due to whitecapping and swell attenuation. This formulation allows WW3 to efficiently resolve  
161 multiple coexisting wave systems, such as locally generated wind seas and remotely generated swells, making it the standard  
162 model for global and basin-scale operational wave forecasting (Alves et al., 2024; Abdolali et al., 2024).

163 For coastal applications, WW3 explicitly resolves shallow-water processes that become dominant as waves propagate  
164 shoreward, including depth-induced breaking, nonlinear triad interactions, and wave refraction over variable bathymetry



165 (Abdolali et al., 2020). To address complex nearshore environments, the model includes advanced source terms, most notably  
166 a wave-vegetation interaction sink term that directly computes wave energy dissipation based on vegetation characteristics  
167 such as stem height, diameter, and density (Abdolali et al., 2022). These physics are critical for modern operational forecasting  
168 systems, including UFS, where an accurate representation of the sea state is essential for high-fidelity coupled predictions  
169 (Abdolali et al., 2021).

170 A major paradigm shift in multi-scale wave modeling was achieved through the implementation of an unstructured triangular  
171 mesh framework coupled with a domain-decomposition (DD) parallelization algorithm (Abdolali et al., 2020). Unlike  
172 traditional explicit numerical schemes, which are strictly constrained by the Courant-Friedrichs-Lewy (CFL) condition, where  
173 the smallest coastal grid cell dictates the global time step, WW3's optional implicit solver relaxes this limitation, enabling  
174 efficient integration at very high spatial resolutions (on the order of 10-50 m). The DD algorithm further improves  
175 computational scalability by optimizing load balancing across thousands of processors, allowing variable-resolution meshes  
176 that smoothly transition from the deep ocean (5-30 km) to complex coastal regions without the computational overhead  
177 associated with traditional nesting approaches, while maintaining high efficiency offshore and resolving sharp coastal gradients  
178 (Abdolali et al., 2026).

179 To resolve total water-level dynamics, WW3 is embedded within coupled modeling frameworks using ESMF. As demonstrated  
180 by (Moghimi et al., 2020a), this coupling enables two-way exchanges between WW3 and hydrodynamic models such as  
181 ADCIRC, whereby currents and water levels modulate wave evolution and wave-induced radiation stresses or vortex forces  
182 feed back into nearshore circulation. In river-estuary-coastal transition zones, this integrated modeling approach is essential;  
183 (Bakhtyar et al., 2020) showed that accurate inundation predictions require the combined effects of river discharge, tides, storm  
184 surge, and waves to be resolved consistently, ensuring a comprehensive assessment of coastal flood hazards.

### 185 **2.1.3 CICE**

186 The CICE is a multi-categorical sea ice model (Hunke et al., 2017) which is used to model the dynamic and thermodynamic  
187 properties of sea ice when UFS-WM is applied in high-latitude regions (Rae et al., 2015). Sea ice affects air-sea fluxes, surface  
188 roughness, and momentum transfer between the atmosphere and ocean. There are several parameterizations which are included  
189 in CICE which aim to model these different aspects of the sea ice. When sea water freezes it forms a pure water crystal with  
190 microscopic brine inclusions, in CICE this is modeled with a mush layer thermodynamic model (Feltham et al., 2006). The  
191 material strength of the sea ice is parameterized using several different rheologies (Hunke et al., 1997; Hunke, 2001; Hunke et  
192 al., 2002). Parameterizations of ice ridging (Lipscomb et al., 2007), melt pond physics (Flocco and Feltham, 2007; Hunke et  
193 al., 2013) and land-fast ice (Lemieux et al., 2016) are also used within CICE. In the UFS, CMEPS manages the exchange of  
194 sea ice concentration, thickness, and other state variables between CICE and the ocean models, such as SCHISM.



## 195 **2.2 the UFS-Coastal component descriptions**

196 While the UFS-WM was designed for global and regional weather prediction, the UFS-Coastal (Fig. 1) adapts the system for  
197 environments where coastal flooding, estuarine circulation, and wave-current interactions are critical. This is achieved by  
198 adding caps in each individual coastal ocean model to work on unstructured/structured grids, allowing flexible resolution in  
199 regions with complex coastlines, wetlands, and nearshore bathymetry.

200 These atmospheric fields (including surface winds, pressure, heat fluxes, and precipitation etc.) are ingested through CDEPS,  
201 maintaining consistency with the UFS-WM's data handling conventions while simplifying the workflow for regional coastal  
202 applications.

203 The UFS-Coastal retains the CMEPS coupling infrastructure, which manages real-time exchanges between the coastal ocean  
204 models, and WW3. This allows for two-way coupling between waves and coastal circulation, where wave radiation stress can  
205 influence nearshore currents and water levels, and evolving currents and water levels modify how waves propagate, break, and  
206 dissipate.

### 207 **2.2.1 ADCIRC**

208 ADCIRC is a finite-element, unstructured-grid hydrodynamic model that can be run either as a two-dimensional depth  
209 integrated (2DDI) model or as a three-dimensional (3D) model designed for simulating tidal dynamics, storm surge, and coastal  
210 flooding (Luettich and Westerink, 2004; Westerink et al., 2008; Hope et al., 2013). Its ability to represent large areas, such as  
211 entire coastlines or ocean basins, while also resolving small-scale features like inlets, levees, and estuarine channels, makes it  
212 particularly useful for storm surge forecasting and flood risk assessment.

213 ADCIRC has been extensively used in both research and operational environments, particularly for hurricane response (e.g.,  
214 Hurricane Surge On-demand Forecast System, HSOFS), where it simulates the combined effects of storm surge, tides, and  
215 wave setup.

### 216 **2.2.2 FVCOM**

217 FVCOM is a depth-resolving unstructured-grid, finite-volume 3D hydrodynamic model designed to simulate tidal and  
218 estuarine circulation, nearshore dynamics, and particle transport (Chen et al., 2006; Chen et al., 2013). Its finite-volume  
219 formulation ensures accurate local conservation of mass and momentum, making it well-suited for environments with complex  
220 shorelines, irregular bathymetry, and strong tidal currents. FVCOM is commonly applied in studies of tidal flushing, estuarine  
221 exchange, and pollutant transport, and is often used to investigate how tides, river discharge, and winds drive circulation and  
222 mixing in estuaries and bays (Sun et al., 2016).



### 223 **2.2.3 SCHISM**

224 SCHISM is another depth-resolving unstructured-grid baroclinic/barotropic hydrodynamic model designed to handle cross-  
225 scale coastal modeling problems, from shelf circulation to wetting and drying in tidal wetlands and floodplains (Zhang and  
226 Baptista, 2008; Zhang et al., 2016). Its dynamic core uses finite-element/finite-volume hybrid methods to efficiently solve the  
227 3D shallow-water equations. Combined with its flexible grid in both the horizontal as well as the vertical dimension, and its  
228 efficient semi-implicit solver, it is capable of providing fine resolution in critical areas while maintaining reasonable  
229 computational cost for larger domains (i.e. ‘seamless’ cross-scale applications), without stringent requirement for mesh quality.  
230 Unlike most other ocean models, SCHISM does not practice bathymetry smoothing or manipulation, and is thus able to  
231 faithfully capture one of the most fundamental drivers of coastal and nearshore processes (Zhang et al., 2024).

232 One of SCHISM’s strengths similar to the other coastal models is its ability to represent wetting and drying processes, which  
233 are critical for simulating coastal inundation, barrier island flooding, and tidal marsh evolution, as demonstrated by its in  
234 NOAA 3-D Surge and Tide Operational Forecast System (STOFS-3D). SCHISM with the biogeochemistry (BGC) capability  
235 and data assimilation (DA) is particularly well-suited for scenarios where water levels fluctuate across intertidal zones,  
236 floodplains, and estuarine wetlands, such as during storm surge events.

### 237 **2.2.4 ROMS**

238 ROMS (Regional Ocean Modelling System) is a 3D structured-grid hydrodynamic model that uses terrain-following vertical  
239 coordinates, making it well-suited for simulating processes where vertical stratification and mixing play important roles.  
240 ROMS is commonly used to study continental shelf circulation, upwelling and downwelling, and cross-shelf transport.  
241 (Shchepetkin and McWilliams, 2005; Moore et al., 2011)

242 ROMS’ vertical grid flexibility and extensive turbulence closure options allow it to capture density-driven flows, such as river  
243 plumes interacting with shelf currents, as well as vertical mixing caused by tides and winds, which makes ROMS useful for  
244 studies of nutrient and sediment transport, as well as applications that involve physical-biogeochemical coupling with DA.

245 UFS-Coastal’s ability to select from these four coastal models (ADCIRC, FVCOM, SCHISM, and ROMS) allows users to  
246 choose the most appropriate tool for the scientific or operational application at hand. By leveraging externally provided  
247 atmospheric forcing and maintaining dynamic coupling with CICE and WW3, the UFS-Coastal ensures that sea ice, wave,  
248 circulation, and flooding processes are represented consistently across all components.

### 249 **2.3 Wave-Current Coupling Methods**

250 Wave-current interaction plays an important role in the storm surge simulations with context-dependent spatial and temporal  
251 impacts on the total water level result (Warner et al., 2010; Sheng et al., 2010; Moghimi et al., 2013; Sun et al., 2013; Kerr et  
252 al., 2013; Garzon and Ferreira, 2016; Moghimi et al., 2020; Martins et al., 2022). UFS-Coastal provides two distinct wave-  
253 current coupling methods for transferring momentum and energy between wave and ocean circulation models: the Longuet-



254 Higgins radiation stress formulation (Longuet-Higgins and Stewart, 1962, 1964) and the 3D vortex formalism(Uchiyama et  
255 al., 2010; Kumar et al., 2012). Both methods enable explicit representation of wave-induced effects within ocean circulation  
256 models but differ fundamentally in their implementation and level of complexity.

### 257 **2.3.1 Longuet-Higgins Radiation Stress Coupling**

258 The Longuet-Higgins radiation stress coupling method represents wave-induced currents and coastal water level setup through  
259 radiation stress gradients formulation (Longuet-Higgins and Stewart, 1962, 1964). In this formulation, WW3 computes wave  
260 properties, such as significant wave height, wave period, and wave direction, and radiation stresses are evaluated from the  
261 computed wave energy density(Moghimi et al., 2020a). These radiation stress terms are then passed directly to the coastal  
262 ocean model (SCHISM here as a case study), where they serve as surface forcing terms in the horizontal momentum equations.  
263 Consequently, the ocean model is able to simulate nearshore currents, wave setup, and associated coastal processes induced  
264 by wave action. The details are in S1.

265 In return, the ocean model provides WW3 with essential hydrodynamic fields, specifically water elevations and surface  
266 horizontal velocities, necessary for WW3 to accurately simulate wave transformation, refraction, and breaking. This two-way  
267 exchange ensures that wave propagation and wave-induced hydrodynamic responses are consistently represented across both  
268 models.

269 This coupling approach is suitable for scenarios where wave-induced nearshore processes are predominantly depth-integrated  
270 and surface-dominated, such as coastal inundation and storm surge modeling.

### 271 **2.3.2 Three-Dimensional Vortex Coupling**

272 In contrast, the 3D vortex coupling method equation explicitly represents the vertical distribution of wave-induced momentum  
273 transfer and mixing processes within the hydrodynamic model (Uchiyama et al., 2010; Bennis et al., 2011; Kumar et al., 2012).  
274 Rather than relying solely on surface-based radiation stresses, this approach accounts for wave-induced momentum fluxes  
275 throughout the entire water column, enabling realistic representation of vertical current shear, wave-induced turbulence, and  
276 wave-enhanced mixing in coastal and estuarine regions.

277 To facilitate this detailed coupling, WW3 exports several phase-averaged wave variables to SCHISM via CMEPS. These  
278 include eastward and northward Stokes drift currents, wave-induced Bernoulli head pressure, near-bottom wave orbital  
279 velocities, wave number and direction, total wave energy, and surface and bottom wave-induced stresses (Table S1). SCHISM  
280 utilizes these detailed wave parameters internally to calculate 3D momentum forcing terms and turbulence parameters  
281 associated with wave-induced vortex forces.

282 Additionally, SCHISM exports hydrodynamic fields back to WW3 via CMEPS, such as sea surface elevation, surface and  
283 depth-averaged velocities, surface Doppler velocities, and a wet/dry cell mask (Table S2). These variables allow WW3 to  
284 accurately represent wave conditions influenced by coastal currents, varying water levels, and wetting/drying processes. The  
285 details are in S2.



286 This comprehensive coupling method is particularly advantageous for modeling scenarios where wave-current interactions  
287 exhibit pronounced vertical variability, influencing sediment transport, vertical mixing, and estuarine circulation dynamics.  
288 By offering both the Longuet-Higgins radiation stress approach and the vertically explicit 3D vortex approach, the UFS-  
289 Coastal provides users with the flexibility to select the coupling methodology best aligned with their scientific goals and  
290 computational resources, when using SCHISM.

## 291 **2.4 Regression System**

292 The UFS-Coastal regression testing (RT) framework plays an essential role in ensuring that model updates, code modifications,  
293 and new developments do not negatively affect model stability, scientific accuracy, or reproducibility. Given the complexity  
294 and modular nature of UFS-Coastal, systematic testing is vital for detecting unintended changes in model performance or  
295 results over different High Performance Computing System (HPCS). The regression system employs automated scripts and  
296 continuous integration practices to regularly verify that the model's scientific and numerical outputs remain consistent over  
297 time.

298 The regression system is based on a suite of predefined test cases representing various coastal and estuarine conditions, from  
299 simplified idealized scenarios to realistic storm events and high-resolution coastal domains. These test cases validate the  
300 performance and interaction of the different coupled components (ADCIRC, FVCOM, SCHISM, ROMS, CICE and WW3)  
301 under conditions relevant to coastal modeling, which are available from the the UFS-Coastal Github page and Zenodo. The  
302 abbreviation used for ADCIRC, FVCOM, SCHISM, ROMS in the RT system are ADC, FVC, SCH and ROM.

### 303 **2.4.1 RT Script Operation**

304 The primary tool for running regression tests is the automated script known as `rt.sh`. This script includes the testing process  
305 from model compilation, configuration and execution to comparing simulation outputs with established baseline datasets.  
306 Specifically, `rt.sh` prepares input files, initializes model components, compiles the codes, executes simulations, and compares  
307 critical model output variables and log files against previously validated reference solutions.

308 If outputs from a regression test exceed predefined tolerance limits compared to the baseline, `rt.sh` identifies and flags these  
309 deviations to the log files. This alerts developers to potential issues quickly, facilitating immediate investigation and resolution,  
310 thus maintaining the reliability of ongoing model development. The UFS-Coastal `rt.sh` has been tested on HPCS from Texas  
311 Advanced Computing Center (TACC), NOAA's Research and Development High Performance Computing Program  
312 (RDHPCS), NOAA's Weather and Climate Operational Supercomputing System (WCOSS), Mississippi State University  
313 (MSU) and the Parallel Works.

### 314 **2.4.2 Workflow**

315 The UFS-Coastal Application (UFS-Coastal-App) workflow (<https://github.com/oceanmodeling/ufs-coastal-app>) is built on  
316 the Unified Workflow Tools (uwtools), an open-source Python package developed for UFS applications, with dedicated drivers



317 for SCHISM and WW3. The workflow uses YAML-based configuration files with Jinja2 template rendering and JSON  
318 Schema validation, and interfaces with the Rocoto workflow manager for task scheduling and dependency management on  
319 HPCS.

320 The workflow automates the key steps of a coupled coastal simulation: building model executables, generating component-  
321 specific configuration and namelist files, staging input data and mesh files, executing the coupled model, and collecting output.  
322 Users specify domain settings, forcing datasets, coupling intervals, and component-specific options through a single YAML  
323 configuration file, from which uwtools generates all necessary model inputs. Further details and practical examples are  
324 available in the UFS-Coastal Application documentation (<https://ufs-coastal-application.readthedocs.io>).

### 325 **2.4.3 Continuous Integration and Continuous Deployment (CI/CD)**

326 CI/CD practices are adopted within the UFS-Coastal development process to systematically integrate and validate model  
327 changes. The automated regression testing pipeline is managed using the Jenkins automation server (The Jenkins Project,  
328 2024), deployed specifically on MSU's Hercules. Jenkins automatically triggers the execution of `rt.sh` regression tests nightly  
329 and whenever new code commits or merges occur in the repository.

330 The test script compiles the model, executes predefined test cases using either Rocoto (Harrop, 2015) for job scheduling, and  
331 compares outputs against archived baseline solutions stored in Amazon Web Services (AWS) S3 cloud storage. Deviations  
332 exceeding predefined tolerances are flagged automatically. Lightweight build and integration checks are additionally  
333 performed through GitHub Actions. The regression tests are validated with both Intel and GNU compilers. By continuously  
334 monitoring the UFS-Coastal codebase, Jenkins on Hercules ensures rapid detection of numerical inconsistencies,  
335 computational instability, or scientific deviations, providing immediate feedback to developers.

### 336 **2.3.4 Regression Test Suite and Configuration**

337 The regression test suite comprises a comprehensive set of standardized scenarios designed to validate both realistic and  
338 idealized coastal modeling applications within the UFS-Coastal. These tests include storm surge simulations, estuarine  
339 circulation scenarios, wave-current interaction studies, and simplified hydrodynamic benchmarks. Each scenario evaluates  
340 interactions within hydrodynamic models (ADCIRC, FVCOM, SCHISM, ROMS) or with the spectral wave model (WW3),  
341 ensuring robust functionality of the CMEPS-based coupling infrastructure. The current status and detailed description of the  
342 test cases can be accessed via the UFS-Coastal repository wiki page on GitHub (<https://github.com/oceanmodeling/ufs-weather-model/wiki>).

344 The test suite systematically verifies component functionality, coupling consistency, and model reliability across diverse  
345 forcing scenarios. It evaluates model stability, numerical accuracy, and computational efficiency across various configurations  
346 and computing architectures.

347 Baseline simulations for all RT cases are systematically archived in an AWS S3 cloud storage bucket. This structured archival  
348 system facilitates efficient and transparent comparisons between historical and current simulation outputs. Whenever



349 discrepancies arise, they are flagged automatically, prompting a detailed review by developers. Such reviews determine  
350 whether differences represent expected numerical variability or indicate issues requiring immediate corrective actions.  
351 This automated and structured regression testing approach significantly enhances scientific rigor, computational stability, and  
352 transparency, reinforcing community confidence in the reliability and performance of the UFS-Coastal modeling framework.

## 353 **2.5 UFS-Coastal App**

354 The UFS-Coastal-App is a comprehensive framework developed to facilitate coastal and regional-scale coupled modeling  
355 simulations within the UFS-Coastal. It is different from the RT system, as RT requires fast computation, the UFS-Coastal-App  
356 is for comprehensive large domain cases. This integration allows for flexible and modular configuration, enabling users to  
357 select the most appropriate modeling components based on specific scientific objectives and regional modeling requirements.  
358 A key feature of the UFS-Coastal-App, as a part of UFS-Coastal is its standardized modeling workflow, encompassing model  
359 setup, input data processing, execution, and output post-processing. This structured workflow supports efficient deployment  
360 and reproducibility across multiple HPCS platforms, facilitating ease of use and consistency in modeling practices. The  
361 application's design provides flexibility in specifying key modeling parameters, such as computational domains, spatial  
362 resolutions, coupling intervals, and model-specific physics options, allowing users to tailor simulations precisely to their  
363 coastal and estuarine modeling needs as a template.

364 Additionally, the UFS-Coastal-App includes comprehensive documentation that guides users through installation,  
365 configuration, model execution, and data management steps, making the tool more accessible to a broad range of coastal  
366 scientists, operational forecasters, and stakeholders. Practical examples of larger-domain and operational-scale coastal  
367 modeling applications are provided within the UFS-Coastal-App repository (<https://github.com/oceanmodeling/ufs-coastal-app>),  
368 demonstrating the system's capability and scalability for addressing diverse coastal phenomena, including storm surge,  
369 wave-current interactions, and flooding events at operationally relevant scales.

## 370 **3 Experimental Configurations and Results**

### 371 **3.1 Hurricane Sandy in Duck, North Carolina**

372 To evaluate the UFS-Coastal modeling system comprehensively, a series of experiments were conducted for both large-scale  
373 storm events and small-scale nearshore hydrodynamics. Specifically, we conducted simulations focused on Hurricane Sandy  
374 (2012) storm surge event, complemented by and performed a series of detailed model validation tests in the Duck, NC region,  
375 which will be later used as regression tests.

376 Hurricane Sandy made landfall as a post-tropical cyclone near Atlantic City, New Jersey, on 29 October 2012 (Fig. 2a) (Fanelli  
377 et al., 2013). Sandy's trajectory and extensive geographic scale made it one of the most severe storm surge and coastal flooding  
378 events on record along the U.S. East Coast (Fanelli et al., 2013). Originating as a tropical cyclone in the southwestern Caribbean  
379 Sea, Sandy moved northward parallel to the U.S. Atlantic coastline before sharply turning northwest toward the mid-Atlantic



380 region. The storm's center passed approximately 450 kilometers offshore to the east-northeast of Duck, NC, before making  
381 landfall further north. Sandy's large wind field extended hundreds of kilometers from its center, producing substantial storm  
382 surges, powerful waves, and coastal erosion along extensive stretches of coastline, including the Outer Banks, NC.

383 The Duck, NC coastal region (Fig. 2b) was specifically selected for detailed validation experiments due to its well-documented  
384 observational record (Newberger and Allen, 2007; Moghimi et al., 2013; Martins et al., 2022), maintained by the USACE FRF.  
385 Established in 1977, Duck FRF provides comprehensive observational datasets, including wave characteristics, water-level  
386 measurements, meteorological data, bathymetric surveys, and current profiles (Fig 2b,c). The region is characterized by a gently  
387 sloping sandy beach transitioning smoothly to offshore depths, making it ideal for evaluating coastal wave transformations,  
388 storm-induced currents, and water-level changes.

389 A systematic set of numerical simulations was conducted for the Duck region, driven by atmospheric forcing consisting of  
390 spatially homogeneous but temporally varying wind velocities and atmospheric pressures obtained from observational  
391 measurements by the "FRF 26m Array" operated by the USACE Coastal Observation and Analysis Branch (COAB) (Fig.  
392 3b,c). The maximum wind speed appeared on October 29, 2012, 00:00 UTC in the Duck region. The atmospheric forcing data  
393 (wind and pressure) in these experiments was provided through CDEPS and was integrated with both WW3 and SCHISM via  
394 CMEPS, facilitating consistent data exchange and coupling.

395 Experiments conducted (Table 1) at Duck included:

- 396 (1) Wave simulations using WW3(ATM+WW3) (Case #1&2),
- 397 (2) Hydrodynamic simulations using SCHISM (ATM+SCH) (Case #3), and
- 398 (3) Fully two-way coupled wave-current simulations integrating SCHISM and WW3 (ATM+SCH+WW3), using two  
399 distinct wave-current coupling methodologies: the traditional Longuet-Higgins radiation stress method (Case #4) and the  
400 advanced 3D vortex coupling approach (Case #5).

401 All of the Duck experiments utilized a common unstructured computational mesh consisting of 23,018 nodes and 46,034  
402 triangular elements for both SCHISM and WW3 (Fig. 2b). The spatial resolution ranged from approximately 45 m near the  
403 shoreline to roughly 1500 m offshore. Observationally derived atmospheric forcing from Duck FRF data (Fig. 3b,c) was  
404 uniformly applied spatially and varied temporally to provide realistic and consistent simulation conditions for detailed model  
405 validation. The timespan of all experiments (Case #1-5) was 2.33 days, from October 27, 2012, 00:00 UTC to October 29,  
406 2012, 04:00 UTC, which covers the passage of Hurricane Sandy over the study region

### 407 **3.2 Experiments**

408 A systematic series of numerical experiments (Table 1) were performed to comprehensively evaluate the predictive capabilities  
409 of the UFS-Coastal modeling system for the Duck region. These experiments incrementally validated individual model  
410 components as well as their coupled effects. Each experiment utilized the consistent computational mesh, observational  
411 datasets, and observational atmospheric forcing conditions that were described in Section 3.1. The following subsections detail  
412 the experimental setups, validation processes, and rationale for each set of comparisons.



### 413 **3.2.1 ATM + WW3**

414 The initial experiments specifically evaluated the wave modeling performance of WW3, driven by observational atmospheric  
415 forcing. The primary objective was to assess WW3's capability to predict key wave parameters, including significant wave  
416 heights, wave periods, and directional spectra, under realistic coastal conditions. Establishing a reliable wave-modeling  
417 baseline was critical, as accurate wave predictions are essential for successful coupled wave-current simulations.

418 The differences of Case 1&2 is that the CDEPS provided the water elevation at FRF8m (Fig.2c, Fig. 3a) via CMEPS to WW3  
419 in Case 2, while no water elevation forcing is used in Case 1. Simulations conducted with WW3 were extensively validated  
420 against wave buoy observations collected at the Duck FRF site. The rationale for this validation was to ensure WW3 accurately  
421 represented nearshore wave processes, enabling subsequent coupled-model experiments to confidently attribute any observed  
422 improvements to explicit wave-current interactions rather than fundamental wave-model performance (Fig. 4).

### 423 **3.2.2 ATM + SCH**

424 The experiments independently validated the SCHISM hydrodynamic model driven by the same observational atmospheric  
425 forcing. The water elevation at FRF8m was used as an open boundary condition here. The purpose of this validation was to  
426 confirm SCHISM's reliability in simulating coastal hydrodynamics-including water-level fluctuations, storm-induced surges,  
427 and nearshore circulation without the influence of wave-induced processes. Establishing SCHISM's standalone accuracy was  
428 crucial for clearly attributing subsequent coupled-model improvements specifically to wave-current interactions.

### 429 **3.2.3 ATM + SCH + WW3 (Longuet-Higgins and vortex Coupling)**

430 The most comprehensive experiment sets involved fully coupled wave-current simulations integrating SCHISM and WW3  
431 under observational atmospheric forcing. This experiment explicitly evaluated two distinct wave-current coupling  
432 methodologies: the widely used Longuet-Higgins radiation stress method and the advanced 3D vortex coupling approach,  
433 previously described in Section 2.2.5.

434 The rationale for comparing these two coupling approaches was to explicitly investigate the advantages of resolving vertical  
435 momentum exchanges and wave-induced turbulence, as well as to evaluate if those formulations were implemented correctly  
436 in the UFS-Coastal. The Longuet-Higgins method served as a well-established benchmark, particularly useful for capturing  
437 surface-driven wave setup and currents. In contrast, the 3D vortex coupling method explicitly resolved vertical wave-induced  
438 momentum transfers and turbulent mixing, potentially offering significant improvements in modeling accuracy for vertically  
439 stratified coastal zones, nearshore circulation, and sediment transport processes.

440 Both coupling approaches utilized identical computational meshes, observational forcing conditions, and initial setups,  
441 ensuring direct comparability. Model outputs (including coastal water levels, wave conditions, and nearshore currents) were  
442 validated against extensive observational datasets from Duck FRF.



### 443 3.3 Results

444 Fig. 4 demonstrated robust agreement between modelled and observed wave characteristics, confirming WW3's standalone  
445 (#1 & #2) accuracy as a critical baseline for further coupled studies. With including water elevation forcing, #2 clearly  
446 improves the significant wave height ( $H_s$ ), especially in the shallower region (Fig. 4 and Table 2). The Longuet-Higgins  
447 method was generally accurate for representing wave-induced setup and flow patterns; however, it inherently lacked the  
448 capability to resolve vertical momentum transfers and associated turbulent mixing. In contrast, the 3D vortex coupling method  
449 captured these vertical complexities, leading to improved accuracy in storm surge predictions, particularly in regions where  
450 vertical gradients in velocity and turbulence are significant. Wave simulations revealed only subtle differences between the  
451 two coupling approaches, especially in the deeper stations, as both effectively reproduced observed nearshore wave conditions.  
452 Nonetheless, during peak storm activity characterized by intensified wave-current interactions, the 3D vortex coupling method  
453 exhibited slightly better skill in capturing wave transformations and energy dissipation processes, reflected in improved  
454 predictions of significant wave height and directional spectra (Fig. 4 and Table 2).

455 Fig.5 was the comparisons between modelled and observed water levels to assess SCHISM's ability to accurately simulate  
456 observed coastal hydrodynamic conditions independently, the results of #3 ensured confidence in its fundamental predictive  
457 performance prior to coupled-model experiments. Comparative evaluations of sea-surface elevations indicated that both  
458 coupling methods effectively captured overall storm surge magnitudes, phase and patterns, ignorable differences between  
459 experiments #3#4 and #5 were shown in all stations due to the small geodomain (Fig. 5).

460 The most substantial improvement from the 3D vortex coupling was evident in the modelled vertical structure of nearshore  
461 currents. Vertical velocity profiles and associated turbulence metrics obtained from the 3D vortex simulations aligned closely  
462 with real observations, capturing the vertical gradients and mixing patterns missing in the Longuet-Higgins approach. Spatial  
463 distributions and vertical cross-sections of simulated current velocities (Fig. 6) provided clear evidence of enhanced realism  
464 and accuracy using the 3D vortex method compared to the depth-integrated approach, highlighting the critical role of vertical  
465 momentum exchanges and turbulence in accurately capturing nearshore hydrodynamics. This vertical resolution is critical for  
466 accurate predictions of sediment transport, pollutant dispersion, and ecological processes in coastal systems.

467 Sensitivity analyses performed on coupling interval frequency and internal model time-step settings indicated clear trade-offs  
468 between computational efficiency and model accuracy. Specifically, shorter coupling intervals and finer internal time-steps  
469 enhanced predictive accuracy, particularly for the 3D vortex coupling method, due to its detailed representation of vertical  
470 processes. However, these improvements came with increased computational costs. Eventually, 300 seconds exchange  
471 frequency is chosen here. Optimal operational configurations thus depend on specific modeling objectives, available  
472 computational resources, and the particular importance of resolving detailed vertical hydrodynamics.

473 In summary, the numerical experiments presented in this section have systematically validated the performance and reliability  
474 of the UFS-Coastal modeling system. Standalone evaluations and fully coupled wave-current simulations at Duck, NC  
475 demonstrated the accuracy and robustness of WW3 and SCHISM, particularly highlighting the advantages of the 3D vortex



476 coupling in capturing complex vertical dynamics in coastal environments. The validation against observational datasets from  
477 Duck FRF confirmed the effectiveness of UFS-Coastal in predicting storm surge, wave conditions, and nearshore circulation.

#### 478 **4 Discussion and conclusion**

479 This study has presented a comprehensive description, systematic validation, and detailed evaluation of the UFS-Coastal  
480 modeling framework (an advanced extension of the UFS-WM) developed specifically to enhance predictions of coastal and  
481 nearshore processes. The core advancement of UFS-Coastal lies in its integration of specialized coastal hydrodynamic models  
482 (SCHISM, ADCIRC, FVCOM, and ROMS), the wave model WW3 and the sea ice model CICE, coupled through the flexible  
483 and modular CMEPS infrastructure, significantly improving predictive capabilities in coastal environments.

484 Experimental validations conducted at Duck, NC, rigorously assessed individual model components as well as their  
485 interactions within fully coupled model configurations. Validation results confirmed robust performance of each modelling  
486 component: WW3 accurately reproduced observed nearshore wave conditions, including significant wave heights and spectral  
487 characteristics, while SCHISM reliably predicted observed coastal water-level variations, storm-induced surges, and nearshore  
488 circulation.

489 A key contribution of this study was the explicit evaluation and comparison of two distinct wave-current interaction  
490 methodologies: the traditional Longuet-Higgins radiation stress formulation and the advanced 3D vortex coupling method.  
491 While both methods successfully captured overall storm surge magnitudes and nearshore wave characteristics, important  
492 distinctions emerged. The depth-integrated Longuet-Higgins approach accurately represented wave-driven coastal setup and  
493 flows, effectively handling scenarios dominated by surface and depth-integrated processes. In contrast, the advanced 3D vortex  
494 coupling provided significant improvements by explicitly resolving vertical momentum transfers and turbulent mixing, leading  
495 to enhanced realism in modeling vertical current structures, mixing processes, and vertical gradients critical for sediment  
496 transport, pollutant dispersion, and ecological modeling.

497 Sensitivity analyses conducted in this study further provided practical guidance regarding optimal model configuration,  
498 explicitly addressing the balance between predictive accuracy and computational efficiency, particularly when applying the  
499 computationally intensive 3D vortex coupling approach.

500 Moving forward, the development roadmap for UFS-Coastal includes several key enhancements to further expand its  
501 predictive capabilities and usability:

502 (1) Future developments will incorporate fully dynamic atmospheric coupling by integrating the atmospheric model  
503 Geophysical Fluid Dynamics Laboratory (GFDL) Finite Volume Cubed-Sphere Dynamical Core (FV3) within the UFS-  
504 Coastal, replacing the current simplified observational atmospheric forcing. This enhancement will enable more realistic  
505 representation of air-sea-wave interactions during rapidly evolving storm conditions.



506 (2) The UFS-Coastal also plans to integrate advanced biogeochemical and ecological modeling components, enabling the  
507 system to address a broader array of coastal issues, such as hypoxia prediction, harmful algal blooms, ecosystem health  
508 assessments, and pollutant transport scenarios.

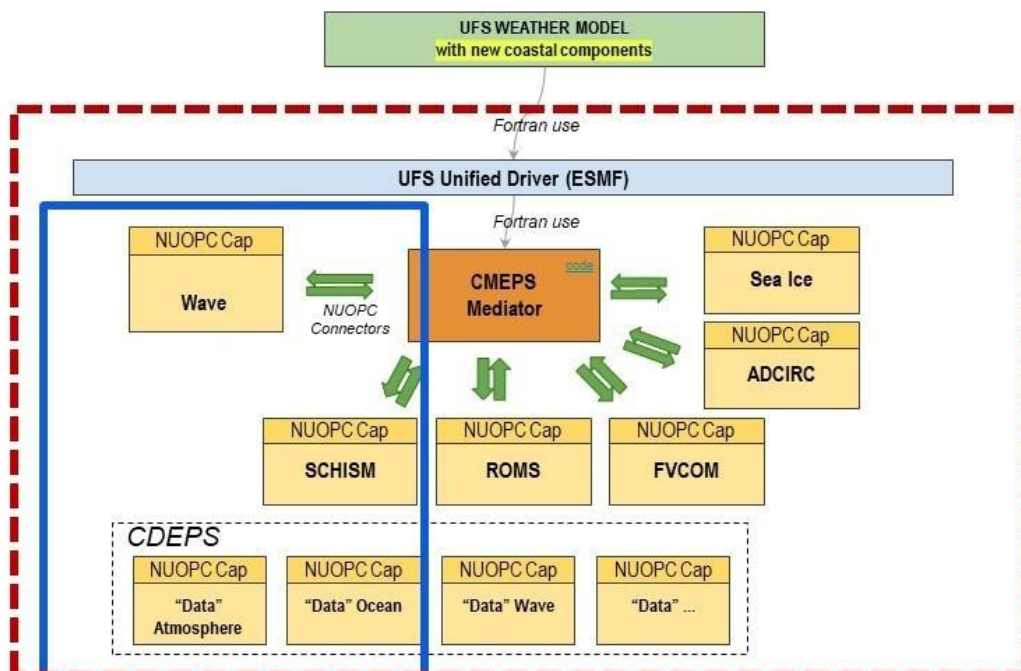
509 (3) The UFS-Coastal will further foster community collaboration through open-source development practices, providing  
510 extensive documentation, training, and user support resources. This community-based approach will encourage wider  
511 adoption, shared innovation, and ongoing improvement from the broader scientific and operational forecasting communities.  
512 In summary, the UFS-Coastal presents substantial advancements in both scientific understanding and practical forecasting  
513 capability compared to existing coastal modeling frameworks. Its modular structure, advanced 3D wave-current interaction  
514 capabilities, demonstrated scalability, and clearly defined roadmap for continuous enhancement firmly establish it as a vital  
515 predictive tool for coastal scientists, resource managers, and operational forecasting agencies.

516



517 **Figure and Tables**

518



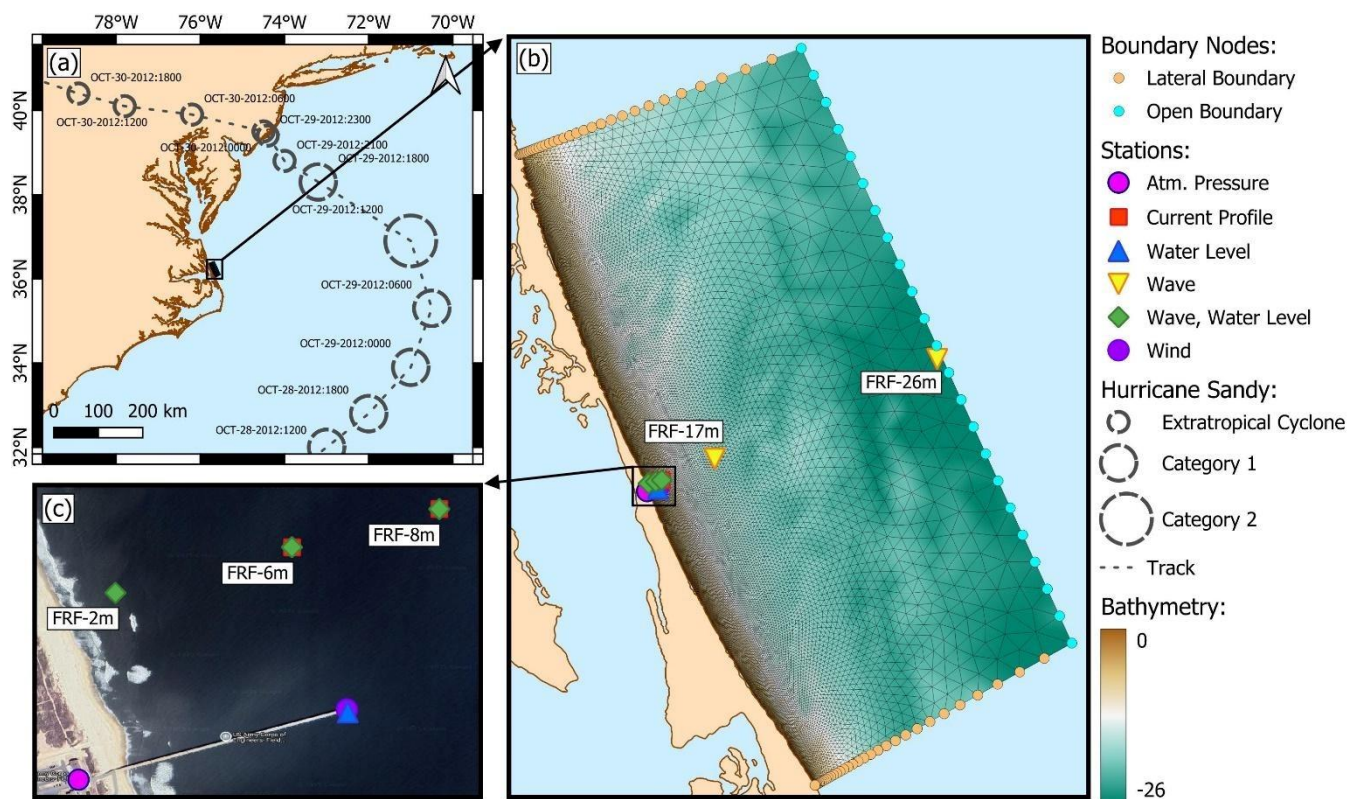
519

520 Figure 1. The UFS-Coastal modeling system architecture (the red dash box), the components in the blue box are the models  
521 used in this study.

522



523



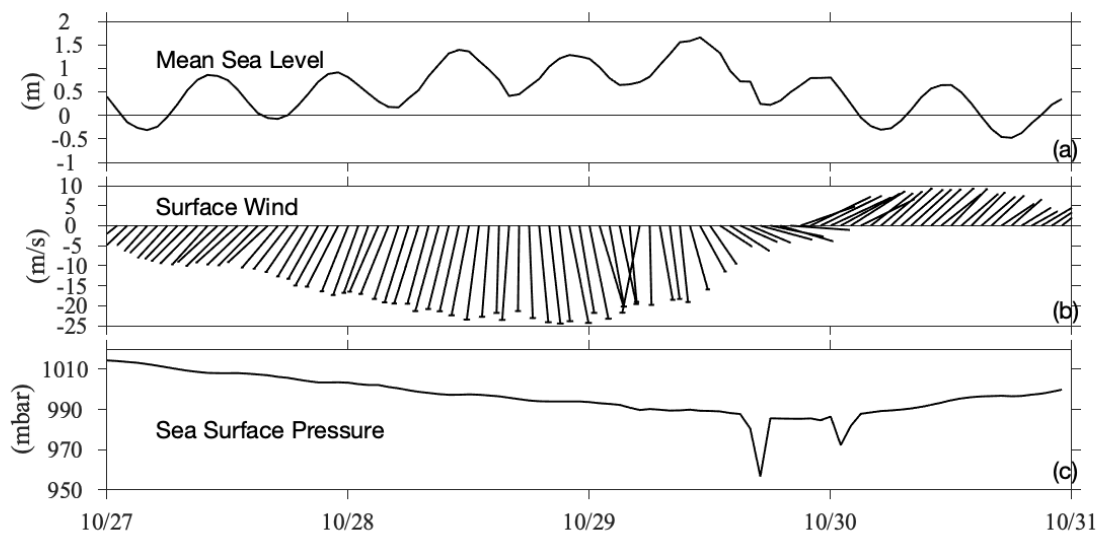
524

525 Figure 2. Hurricane Sandy's track is shown in (a), the study region Duck, NC is shown with the zoom in (a) and zoomed out  
 526 view (b) of the unstructured triangular mesh. The unstructured grid consists of 23,018 nodes and 45,167 elements, with  
 527 depths represented by the color scale (in meters), (c) zoom in the box in (b). The mesh demonstrates increased resolution  
 528 near the coastline and areas of interest while maintaining computational efficiency with coarser resolution in the offshore  
 529 regions. The observation stations are labelled in (b) and (c). Coastlines in (a) and (b) use the Global Self-consistent,  
 530 Hierarchical, High-resolution Geography Database (GSHHG, <https://www.ngdc.noaa.gov/mgg/shorelines/shorelines.html>).  
 531 Hurricane Data in (a) is from the International Best Track Archive for Climate Stewardship  
 532 (IBTrACS, <https://www.ncei.noaa.gov/products/international-best-track-archive>). Basemap in (c) is using Google Maps  
 533 Satellite Imagery.

534



535



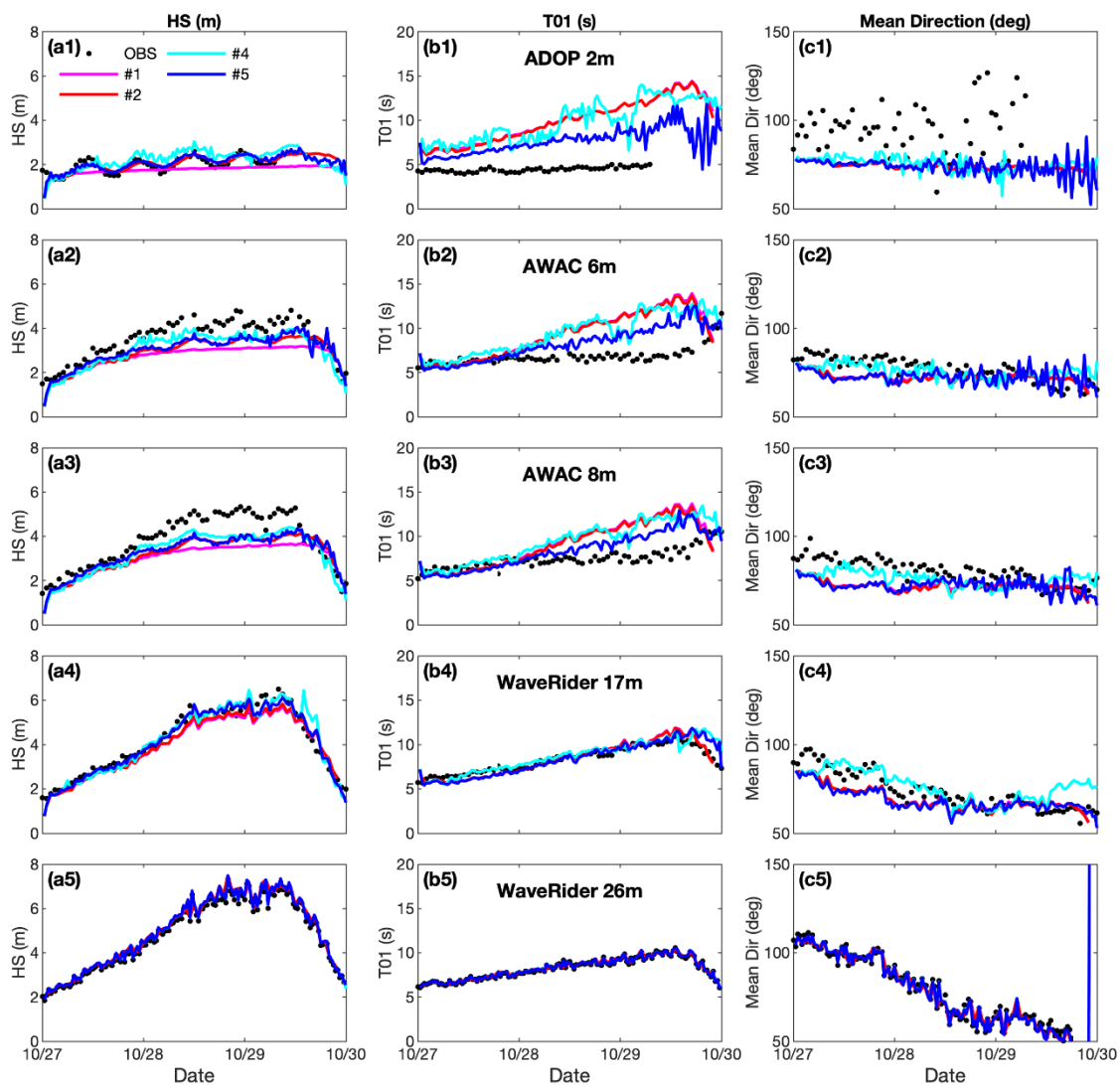
536

537 Figure 3. The observed atmospheric and oceanic forcing during the passage of Hurricane Sandy in the Duck, NC

538



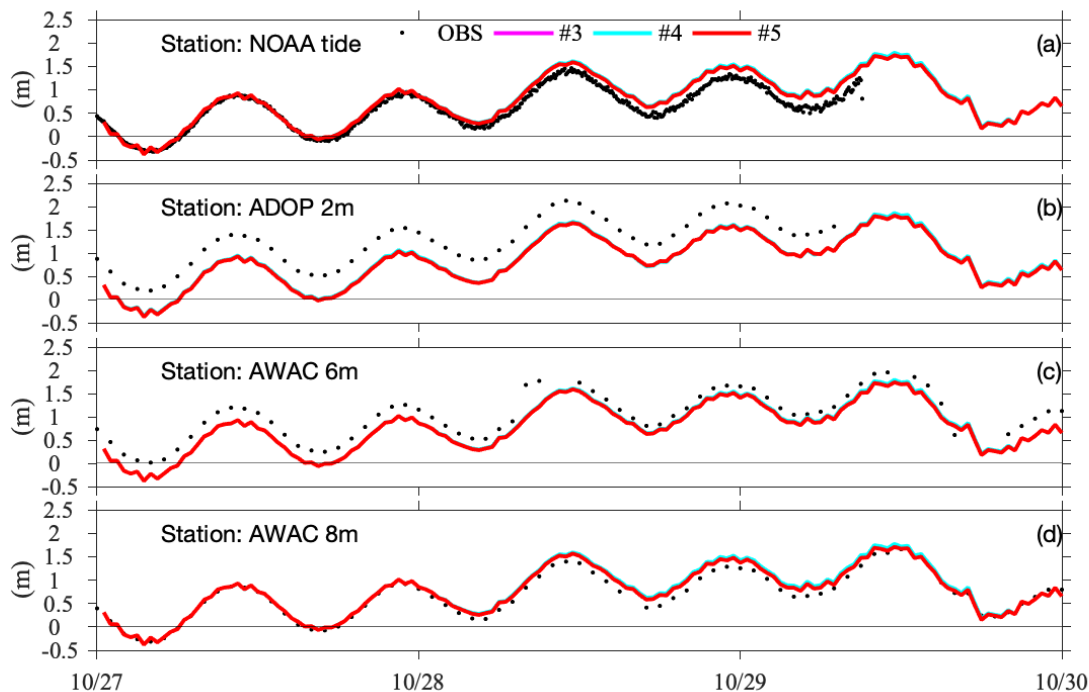
539



540

541 Figure 4. Significant wave height, Mean time period, and mean direction comparisons between observations and numerical  
542 experiments #1, #2, #4, #5. The 5 stations are shown in Fig. 2.

543



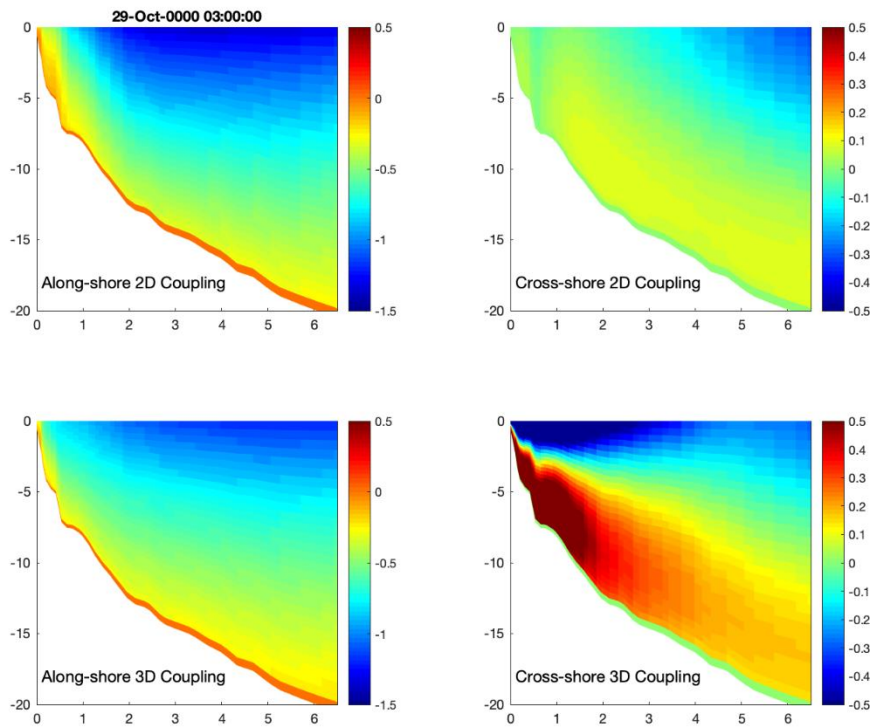
544

545 Figure 5. Water elevation comparisons between observations and numerical experiments #3, #4, #5. The 4 stations are  
546 shown in Fig. 2.

547



548



549

550 Figure 6. The along shore and cross shore velocity components from coast to awac6m station at the time of 03:00 October 29  
551 2012 as a typical scenario.

552



553 **Table 1. Details about the 6 experiments**

Case	Components	Details
#1	ATM+WW3	Without water elevation forcing
#2	ATM+WW3	With water elevation forcing
#3	ATM+SCH	
#4	ATM+SCH+WW3	Longuet-Higgins Radiation Coupling
#5	ATM+SCH+WW3	3D Vortex Coupling

554 **Table 2. Statistics of the wave parameter between the observation and experiments, Significant wave height (Hs), Mean period (T01),**  
 555 **Mean direction (Dir), Root Mean Square Error (RMSE), Mean Absolute Error (MAE)**  
 556

Instrument	Variable	#1			#2			#4			#5		
		Bias	RMSE	MAE	Bias	RMSE	MAE	Bias	RMSE	MAE	Bias	RMSE	MAE
ADOP 2m	HS	-0.25	0.38	0.30	0.00	0.20	0.17	0.20	0.39	0.33	0.04	0.20	0.15
	T01	4.63	4.92	4.63	4.58	4.89	4.58	4.60	4.94	4.60	2.76	2.90	2.76
	Dir	-19.40	24.03	19.98	-19.66	24.23	20.22	-18.26	22.50	18.80	-19.62	23.52	20.01
AWAC 6m	HS	-0.85	0.97	0.86	-0.64	0.75	0.67	-0.50	0.55	0.50	-0.53	0.66	0.58
	T01	2.63	3.51	2.78	2.52	3.40	2.68	2.55	3.19	2.58	1.43	2.09	1.64
	Dir	-3.96	7.08	6.05	-4.48	7.35	6.29	-1.00	6.39	5.23	-3.95	8.08	6.88
AWAC 8m	HS	-0.85	1.05	0.89	-0.66	0.84	0.74	-0.55	0.67	0.56	-0.56	0.78	0.65
	T01	1.85	2.74	2.17	1.73	2.63	2.07	1.98	2.52	2.05	0.93	1.66	1.29
	Dir	-7.82	9.75	8.38	-8.41	10.16	8.88	-4.22	7.32	6.49	-7.80	10.09	8.69
WaveRider 17m	HS	-0.26	0.41	0.34	-0.22	0.37	0.31	0.01	0.40	0.27	-0.04	0.26	0.19
	T01	0.05	0.61	0.50	0.02	0.59	0.48	0.33	0.81	0.52	0.03	0.74	0.55
	Dir	-4.41	7.22	5.89	-4.81	7.39	6.10	2.63	7.90	6.21	-5.19	7.93	6.56
WaveRider 26m	HS	0.13	0.13	0.13	0.13	0.13	0.13	0.12	0.13	0.12	0.12	0.14	0.13
	T01	0.05	0.08	0.06	0.05	0.08	0.06	0.05	0.10	0.07	0.04	0.10	0.07
	Dir	-0.63	2.25	1.52	-0.63	2.25	1.52	-0.40	2.77	1.64	-0.60	2.74	1.64
Mean	HS	-0.42	0.59	0.51	-0.28	0.46	0.41	-0.14	0.43	0.36	-0.19	0.41	0.34
	T01	1.84	2.37	2.03	1.78	2.32	1.98	1.90	2.31	1.96	1.04	1.50	1.26
	Dir	-7.24	10.07	8.36	-7.59	10.27	8.60	-4.25	9.37	7.67	-7.43	10.47	8.76

557  
558



559 **Code and data availability**

560 The version of the UFS-Coastal modeling system used in this study, including the workflow, the active model components  
561 (CICE and WW3), and the input files required to reproduce the results presented in this paper, is archived on Zenodo at  
562 <https://doi.org/10.5281/zenodo.18458640> (Sun, 2026) under the Lesser GNU Public License v3. Because the individual  
563 components of the UFS-Coastal system are pinned by Git commit hashes rather than released under independent version  
564 numbers, the exact configuration used here is captured by the single project-level tag v1.0.0b01 This tag records the specific  
565 commit of every component in the coupled system, and the complete list of component repositories and their corresponding  
566 commit hashes is included in the archived release.

567 **Author contributions**

568 YS: conceptualization, methodology, UFS-Coastal code development, workflow development and implementation, data  
569 curation, visualization, validation, writing (original draft). UT: conceptualization, methodology, UFS-Coastal code  
570 development, workflow development and implementation, writing (review and editing). MJ: conceptualization, methodology,  
571 UFS-Coastal code development, workflow development and implementation, writing (review and editing) HY:  
572 conceptualization, methodology, UFS-Coastal code and SCHISM development, workflow development and implementation,  
573 validation. JZ: conceptualization, methodology, UFS-Coastal code and SCHISM development, writing (review and editing).  
574 CL: conceptualization, methodology, UFS-Coastal code and SCHISM development, writing (review and editing). AA:  
575 conceptualization, methodology, UFS-Coastal code and WW3 development, workflow development and implementation, data  
576 curation, writing (review and editing). DW: conceptualization, methodology, UFS-Coastal code and WW3 development. ). IT:  
577 UFS-Coastal project management, writing (review and editing). JH: conceptualization, UFS-Coastal project management,  
578 writing (review and editing). PV: UFS-Coastal code development, writing (review and editing). FC: workflow development  
579 and implementation, visualization, writing (review and editing). SM: workflow development and implementation. FD:  
580 workflow development and implementation, writing (review and editing). SB: WW3 development. AS: WW3 development.  
581 JS: UFS-Coastal: CICE development, writing (review and editing). EM: conceptualization, UFS-Coastal project management.  
582 SM: conceptualization, UFS-Coastal project management, writing (review and editing).

583 **Competing interests**

584 The authors declare that they have no conflict of interest.



## 585 **Disclaimer**

586 The views expressed in this manuscript are solely those of the authors and do not necessarily reflect the official policies or  
587 positions of NOAA, the U.S. Government, or affiliated institutions. Mention of commercial products, software, or services  
588 does not imply endorsement by NOAA or the U.S. Government.

## 589 **Acknowledgements**

590 The authors acknowledge the contributions of the wider UFS-Weather Model community for ongoing model development,  
591 code contributions, and insightful discussions that enhanced the quality and applicability of the UFS-Coastal. The authors also  
592 thank Dr. Atieh Alipour and Dr. Jack Reeves Eyre for internal review and discussions. Simulations used in this paper were  
593 conducted using the NOAA's Research and Development High Performance Computing Systems (RDHPCS), including  
594 HERA - NOAA Environmental Security Computing Center (NESCC) in Fairmont-WV, and HERCULES - Mississippi State  
595 University (MSU) in Starkville-MS.

## 596 **Financial support**

597 This work was supported by funding from the National Oceanic and Atmospheric Administration (NOAA). For VIMS, the  
598 funding sources are: NA23NOS4730238 and NA23NOS4730239. Ali Abdolali acknowledges support from the Coastal  
599 Forecasting to Reduce Infrastructure Flooding Program and the Wave Information Study (WIS) under the USACE Coastal and  
600 Ocean Data System (CODS) Base Program. C.L. was funded by the program Changing Coasts of the Helmholtz Association.  
601 For NCAR, this material is based upon work supported by the NSF National Center for Atmospheric Research, which is a  
602 major facility sponsored by the U.S. National Science Foundation under Cooperative Agreement No. 1852977.

## 603 **References**

604 Abdolali, A., Banihashemi, S., Alves, J. H., Roland, A., Hesser, T. J., Anderson Bryant, M., and Mckee Smith, J.: Great Lakes  
605 wave forecast system on high-resolution unstructured meshes, *Geoscientific Model Development*, 17, 1023-1039,  
606 10.5194/gmd-17-1023-2024, 2024.  
607 Abdolali, A., Hesser, T. J., Roland, A., Schönau, M., Honegger, D. A., Smith, J. M., Michaud, H., and Centurioni, L.:  
608 Advancing multi-scale wave modeling: Global and coastal applications during the 2022 Atlantic hurricane season, *Ocean*  
609 *Modelling*, 199, 10.1016/j.ocemod.2025.102623, 2026.  
610 Abdolali, A., Roland, A., Westhuysen, A. v. d., Meixner, J., Chawla, A., Hesser, T. J., Smith, J. M., and Sikiric, M. D.: Large-  
611 scale hurricane modeling using domain decomposition parallelization and implicit scheme implemented in WAVEWATCH  
612 III wave model, *Coastal Engineering*, 157, 10.1016/j.coastaleng.2020.103656, 2020.  
613 Abdolali, A., Hesser, T. J., Anderson Bryant, M., Roland, A., Khalid, A., Smith, J., Ferreira, C., Mehra, A., and Sikiric, M. D.:  
614 *Frontiers | Wave Attenuation by Vegetation: Model Implementation and Validation Study*, *Frontiers in Built Environment*, 8,  
615 10.3389/fbuil.2022.891612, 2022.



- 616 Abdolali, A., van der Westhuysen, A., Ma, Z., Mehra, A., Roland, A., Moghimi, S., Abdolali, A., van der Westhuysen, A.,  
617 Ma, Z., Mehra, A., Roland, A., and Moghimi, S.: Evaluating the accuracy and uncertainty of atmospheric and wave model  
618 hindcasts during severe events using model ensembles, *Ocean Dynamics* 2021 71:2, 71, 10.1007/s10236-020-01426-9, 2021.
- 619 Alves, J.-H., Padilla-Hernandez, R., Spindler, D., Kolczynski, W., Rajan, B., Spindler, T., Abdolali, A., Campos, R.,  
620 Banihashemi, S., and Meixner, J.: Development of a Wave Model Component in the First Coupled Global Ensemble Forecast  
621 System at NOAA, *Weather and Forecasting*, 39, 1761-1776, 10.1175/waf-d-24-0048.1, 2024.
- 622 Bakhtyar, R., Maitaria, K., Velissariou, P., Trimble, B., Mashriqui, H., Moghimi, S., Abdolali, A., Westhuysen, A. J. V. d.,  
623 Ma, Z., Clark, E. P., and Flowers, T.: A New 1D/2D Coupled Modeling Approach for a Riverine-Estuarine System Under  
624 Storm Events: Application to Delaware River Basin, *Journal of Geophysical Research: Oceans*, 125, 10.1029/2019JC015822,  
625 2020.
- 626 Bennis, A.-C., Arduin, F., and Dumas, F.: On the coupling of wave and three-dimensional circulation models: Choice of  
627 theoretical framework, practical implementation and adiabatic tests, *Ocean Modelling*, 40, 260-272,  
628 10.1016/j.ocemod.2011.09.003, 2011.
- 629 Chen, C., Beardsley, R., and Cowles, G.: An Unstructured Grid, Finite-Volume Coastal Ocean Model (FVCOM) System,  
630 *Oceanography*, 19, 78-89, 10.5670/oceanog.2006.92, 2006.
- 631 Chen, C., Beardsley, R., Cowles, G., Qi, J., Lai, Z., Gao, G., Stuebe, D., Liu, H., Xu, Q., Xue, P., Ge, J., Hu, S., Ji, R., Tian,  
632 R., Huang, H., Wu, L., Lin, H., and Sun, Y.: An Unstructured Grid, Finite-Volume Community Ocean Model  
633 FVCOM User Manual, SMAST/UMASSD-13-0701, 2013.
- 634 COASTAL Act: Consumer Option for an Alternative System to Allocate Losses Act, 112-141, 2012.
- 635 Deb, M., Abdolali, A., Kirby, J. T., and Shi, F.: Hydrodynamic modeling of a complex salt marsh system: Importance of  
636 channel shoreline and bathymetric resolution, *Coastal Engineering*, 173, 10.1016/j.coastaleng.2022.104094, 2022.
- 637 Fanelli, C., Fanelli, P., and Wolcott, D.: Hurricane Sandy 2012 NOAA NOS Water Level and Meteorological Data Report,  
638 NOAA, 2013.
- 639 Feltham, D. L., Untersteiner, N., Wettlaufer, J. S., and Worster, M. G.: Sea ice is a mushy layer, *Geophysical Research Letters*,  
640 33, 10.1029/2006GL026290, 2006.
- 641 Flocco, D. and Feltham, D. L.: A continuum model of melt pond evolution on Arctic sea ice, *Journal of Geophysical Research:*  
642 *Oceans*, 112, 10.1029/2006JC003836, 2007.
- 643 Gröger, M., Dieterich, C., Haapala, J., Ho-Hagemann, H. T. M., Hagemann, S., Jakacki, J., May, W., Meier, H. E. M., Miller,  
644 P. A., Rutgersson, A., and Wu, L.: Coupled regional Earth system modeling in the Baltic Sea region, *Earth System Dynamics*,  
645 12, 939-973, 10.5194/esd-12-939-2021, 2021.
- 646 Harrop, C.: Rocoto Workflow Management System [code], 2015.
- 647 Hersbach, H., Bell, B., Berrisford, P., Hirahara, S., Horányi, A., Muñoz-Sabater, J., Nicolas, J., Peubey, C., Radu, R., Schepers,  
648 D., Simmons, A., Soci, C., Abdalla, S., Abellan, X., Balsamo, G., Bechtold, P., Biavati, G., Bidlot, J., Bonavita, M., De Chiara,  
649 G., Dahlgren, P., Dee, D., Diamantakis, M., Dragani, R., Flemming, J., Forbes, R., Fuentes, M., Geer, A., Haimberger, L.,  
650 Healy, S., Hogan, R. J., Hólm, E., Janisková, M., Keeley, S., Laloyaux, P., Lopez, P., Lupu, C., Radnoti, G., de Rosnay, P.,  
651 Rozum, I., Vamborg, F., Villaume, S., and Thépaut, J. N.: The ERA5 global reanalysis, *Quarterly Journal of the Royal  
652 Meteorological Society*, 146, 1999-2049, 10.1002/qj.3803, 2020.
- 653 Hope, M. E., Westerink, J. J., Kennedy, A. B., Kerr, P. C., Dietrich, J. C., Dawson, C., Bender, C. J., Smith, J. M., Jensen, R.  
654 E., Zijlema, M., Holthuijsen, L. H., Luettich, R. A., Powell, M. D., Cardone, V. J., Cox, A. T., Pourtaheri, H., Roberts, H. J.,  
655 Atkinson, J. H., Tanaka, S., Westerink, H. J., and Westerink, L. G.: Hindcast and validation of Hurricane Ike (2008) waves,  
656 forerunner, and storm surge, *Journal of Geophysical Research: Oceans*, 118, 4424-4460, 10.1002/jgrc.20314, 2013.
- 657 Hunke, E., Lipscomb, W., Jones, P., Turner, A., Jeffery, N., and Elliott, S.: CICE, The Los Alamos Sea Ice Model,  
658 10.11578/dc.20171025.1964, 2017.
- 659 Hunke, E. C.: Viscous-Plastic Sea Ice Dynamics with the EVP Model: Linearization Issues, *Journal of Computational Physics*,  
660 170, 10.1006/jcph.2001.6710, 2001.
- 661 Hunke, E. C., Hebert, D. A., and Lecomte, O.: Level-ice melt ponds in the Los Alamos sea ice model, CICE, *Ocean Modelling*,  
662 71, 10.1016/j.ocemod.2012.11.008, 2013.
- 663 Hunke, E. C., Dukowicz, J. K., Hunke, E. C., and Dukowicz, J. K.: An Elastic-Viscous-Plastic Model for Sea Ice Dynamics,  
664 *Journal of Physical Oceanography*, 27, 10.1175/1520-0485(1997)027, 1997.



- 665 Hunke, E. C., Dukowicz, J. K., Hunke, E. C., and Dukowicz, J. K.: The Elastic Viscous Plastic Sea Ice Dynamics Model in  
666 General Orthogonal Curvilinear Coordinates on a Sphere—Incorporation of Metric Terms, *Monthly Weather Review*, 130,  
667 10.1175/1520-0493(2002)130, 2002.
- 668 Jacobs, N. A.: Open Innovation and the Case for Community Model Development, *Bulletin of the American Meteorological*  
669 *Society*, 102, E2002-E2011, 10.1175/bams-d-21-0030.1, 2021.
- 670 Kumar, N., Voulgaris, G., Warner, J. C., and Olabarrieta, M.: Implementation of the vortex force formalism in the coupled  
671 ocean-atmosphere-wave-sediment transport (COAWST) modeling system for inner shelf and surf zone applications, *Ocean*  
672 *Modelling*, 47, 65-95, 10.1016/j.ocemod.2012.01.003, 2012.
- 673 Lemieux, J.-F., Dupont, F., Blain, P., Roy, F., Smith, G. C., and Flato, G. M.: Improving the simulation of landfast ice by  
674 combining tensile strength and a parameterization for grounded ridges, *Journal of Geophysical Research: Oceans*, 121,  
675 10.1002/2016JC012006, 2016.
- 676 Lipscomb, W. H., Hunke, E. C., Maslowski, W., and Jakacki, J.: Ridging, strength, and stability in high-resolution sea ice  
677 models, *Journal of Geophysical Research: Oceans*, 112, 10.1029/2005JC003355, 2007.
- 678 Longuet-Higgins, M. S. and Stewart, R. W.: Radiation stress and mass transport in gravity waves, with application to 'surf  
679 beats', *Journal of Fluid Mechanics*, 13, 481-504, 10.1017/S0022112062000877, 1962.
- 680 Longuet-Higgins, M. S. and Stewart, R. W.: Radiation stresses in water waves; a physical discussion, with applications, *Deep*  
681 *Sea Research*, 11, 529-562, 1964.
- 682 Luetlich, R. A. and Westerink, J. J.: Formulation and Numerical Implementation of the 2D/3D ADCIRC Finite Element Model,  
683 University of North Carolina at Chapel Hill & University of Notre Dame, 2004.
- 684 Martins, K., Bertin, X., Mengual, B., Pezerat, M., Lavaud, L., Guérin, T., and Zhang, Y. J.: Wave-induced mean currents and  
685 setup over barred and steep sandy beaches, *Ocean Modelling*, 179, 10.1016/j.ocemod.2022.102110, 2022.
- 686 Moghimi, S., Klingbeil, K., Gräwe, U., and Burchard, H.: A direct comparison of a depth-dependent Radiation stress  
687 formulation and a Vortex force formulation within a three-dimensional coastal ocean model, *Ocean Modelling*, 70,  
688 10.1016/j.ocemod.2012.10.002, 2013.
- 689 Moghimi, S., Vinogradov, S., Myers, E. P., Funakoshi, Y., Van der Westhuysen, A. J., Abdolali, A., Ma, Z., and Liu, F.:  
690 Development of a Flexible Coupling Interface for ADCIRC Model for Coastal Inundation Studies, United States. National  
691 Ocean Service41, 10.25923/akzc-kc14, 2019.
- 692 Moghimi, S., Van der Westhuysen, A., Abdolali, A., Myers, E., Vinogradov, S., Ma, Z., Liu, F., Mehra, A., and Kurkowski,  
693 N.: Development of an ESMF Based Flexible Coupling Application of ADCIRC and WAVEWATCH III for High Fidelity  
694 Coastal Inundation Studies, *Journal of Marine Science and Engineering*, 8, 10.3390/jmse8050308, 2020a.
- 695 Moghimi, S., van der Westhuysen, A., Abdolali, A., Myers, E., Vinogradov, S., Ma, Z., Liu, F., Mehra, A., and Kurkowski,  
696 N.: Development of a Flexible Coupling Framework for Coastal Inundation Studies, 10.48550/arXiv.2003.12652, 2020b.
- 697 Moore, A. M., Arango, H. G., Broquet, G., Powell, B. S., Weaver, A. T., and Zavala-Garay, J.: The Regional Ocean Modeling  
698 System (ROMS) 4-dimensional variational data assimilation systems, *Progress in Oceanography*, 91, 34-49,  
699 10.1016/j.pocean.2011.05.004, 2011.
- 700 Newberger, P. A. and Allen, J. S.: Forcing a three-dimensional, hydrostatic, primitive-equation model for application in the  
701 surf zone: 1. Formulation, *Journal of Geophysical Research: Oceans*, 112, 10.1029/2006JC003472, 2007.
- 702 Rae, J. G. L., Hewitt, H. T., Keen, A. B., Ridley, J. K., West, A. E., Harris, C. M., Hunke, E. C., and Walters, D. N.:  
703 Development of the Global Sea Ice 6.0 CICE configuration for the Met Office Global Coupled model, *Geoscientific Model*  
704 *Development*, 8, 2221-2230, 10.5194/gmd-8-2221-2015, 2015.
- 705 Shchepetkin, A. F. and McWilliams, J. C.: The regional oceanic modeling system (ROMS): a split-explicit, free-surface,  
706 topography-following-coordinate oceanic model, *Ocean Modelling*, 9, 347-404, 10.1016/j.ocemod.2004.08.002, 2005.
- 707 Sun, Y.: The applications of UFS-Coastal: Coupling of SCHISM and WAVEWATCH III, 10.5281/zenodo.18458640, 2026.
- 708 Sun, Y., Chen, C., Beardsley, R. C., Ullman, D., Butman, B., and Lin, H.: Surface circulation in Block Island Sound and  
709 adjacent coastal and shelf regions: A FVCOM-CODAR comparison, *Progress in Oceanography*, 143, 26-45,  
710 10.1016/j.pocean.2016.02.005, 2016.
- 711 The Jenkins Project: Jenkins Automation Server (2.440.1), The Jenkins Project [code], 2024.
- 712 The WAVEWATCH III® Development Group (WW3DG): User manual and system documentation of WAVEWATCH III®  
713 version 6.07, NOAA/NWS/NCEP/MMAB, College Park, MD, USATech. Note 333, 326 pp. + Appendices, 2019.



714 Thomas, E. E., Müller, M., Bohlinger, P., Batrak, Y., and Szapiro, N.: A Kilometer-Scale Coupled Atmosphere-Wave  
715 Forecasting System for the European Arctic, *Weather and Forecasting*, 10.1175/waf-d-21-0065.1, 2021.  
716 Uchiyama, Y., McWilliams, J. C., and Shchepetkin, A. F.: Wave–current interaction in an oceanic circulation model with a  
717 vortex-force formalism: Application to the surf zone, *Ocean Modelling*, 34, 16–35, 10.1016/j.ocemod.2010.04.002, 2010.  
718 Field Research Facility: <https://chldata.erdcdren.mil/thredds/catalog/frf/catalog.html>, last  
719 Ward, N. D., Megonigal, J. P., Bond-Lamberty, B., Bailey, V. L., Butman, D., Canuel, E. A., Diefenderfer, H., Ganju, N. K.,  
720 Goñi, M. A., Graham, E. B., Hopkinson, C. S., Khangaonkar, T., Langley, J. A., Mcdowell, N. G., Myers-Pigg, A. N.,  
721 Neumann, R. B., Osburn, C. L., Price, R. M., Rowland, J., Sengupta, A., Simard, M., Thornton, P. E., Tzortziou, M., Vargas,  
722 R., Weisenhorn, P. B., and Windham-Myers, L.: Representing the function and sensitivity of coastal interfaces in Earth system  
723 models, *Nature Communications*, 11, 10.1038/s41467-020-16236-2, 2020.  
724 Westerink, J. J., Luettich, R. A., Feyen, J. C., Atkinson, J. H., Dawson, C., Roberts, H. J., Powell, M. D., Dunion, J. P.,  
725 Kubatko, E. J., and Pourtaheri, H.: A Basin- to Channel-Scale Unstructured Grid Hurricane Storm Surge Model Applied to  
726 Southern Louisiana, *Monthly Weather Review*, 136, 833–864, 10.1175/2007mwr1946.1, 2008.  
727 Worthen, D., Wang, J., Montuoro, R., Heinzeller, D., Li, B., Theurich, G., Turuncoglu, U., Rosen, D., Jovic, D., Curtis, B.,  
728 Mahajan, R., Lei, H., Richert, A., Chawla, A., Wang, J., Meixner, J., Abdolali, a., Masarik, M., Pan, L., Barlage, M., Liu, B.,  
729 Vertensten, M., Craig, t., Benson, R., Robinson, T., Clune, T., Jiang, W., Barton, N., Vandenberghe, G., Potts, M., Kim, J.,  
730 Perlin, N., Book, C., Bernardet, L., Yang, F., Sun, S., Kim, H.-S., Baker, B., Huang, J., Jeon, C.-H., and Stainer, I.: Coupling  
731 Infrastructure Capability in UFS Weather Model, NOAA, 10.25923/dvv2-3g03, 2024.  
732 Zhang, Y. and Baptista, A. M.: SELFE: A semi-implicit Eulerian–Lagrangian finite-element model for cross-scale ocean  
733 circulation, *Ocean Modelling*, 21, 71–96, 10.1016/j.ocemod.2007.11.005, 2008.  
734 Zhang, Y. J., Ye, F., Stanev, E. V., and Grashorn, S.: Seamless cross-scale modeling with SCHISM, *Ocean Modelling*, 102,  
735 64–81, 10.1016/j.ocemod.2016.05.002, 2016.  
736 Zhang, Y. J., Anderson, J., Park, K., Wu, C. H., Wipperfurth, S., Anderson, E., Pe'eri, S., Beletsky, D., Titze, D., Lorenzo, E.  
737 D., Moghimi, S., Seroka, G., Myers, E., Fujisaki-Manome, A., and Kelley, J.: Debunking common myths in coastal circulation  
738 modeling, *Ocean Modelling*, 190, 10.1016/j.ocemod.2024.102401, 2024.  
739